Protective effect of isoflurane preconditioning on neurological function in rats with HIE

Yi-Bo Wang
Jinzhou Medical University
Ting-Bao Chen
Kunming Medical University
Li-Ren Huang-Fu
Kunming Medical University
Hong-Su Zhou
Affiliated Hospital of Zunyi Medical University
Qiu-Xia Xiao
Kunming Medical University
Xu Fang
Affiliated Hospital of Zunyi Medical University
Liu-Lin Xiong
Affiliated Hospital of Zunyi Medical University
Ting-Hua Wang (wangth_email@163.com)
Jinzhou Medical University

Research Article

Keywords: Hypoxic ischemic encephalopathy, Isoflurane, ISO, Anesthesia, Preconditioning

Posted Date: April 18th, 2022

DOI: https://doi.org/10.21203/rs.3.rs-1561903/v1

Abstract

Objective

Hypoxic ischemic encephalopathy (HIE) is an important cause of neonatal death and disability, which can lead to long-term neurological and motor dysfunction. At present, the treatment mainly focuses on the symptomatic treatment in the acute phase and rehabilitation after injury, but the effect is not satisfactory, and more effective methods are urgently needed. Due to the widespread use of inhalation anesthetics in surgery, it has been found that isoflurane (ISO) preconditioning may have a positive effect on neuroprotection. The aim of this study was to investigate the effects of ISO preconditioning on neurological function and behavior in HIE rats.

Methods

Neonatal rats were used to create hypoxic-ischemic (HI) model by ligating the right common carotid artery at 7 days and then in a hypoxia chamber. The effects of anesthetic drugs on neurological function after one hour of ISO preconditioning were assessed after modeling by Morris water maze(MWM), Y-maze, and rotarod tests at one month. Thereafter, samples were taken at 1 and 42 days for Nissl staining and Hematoxylin-Eosin (HE) staining to observe neuronal number and histomorphology changes. The relationship of behaviour and morphology tests were measured.

Results

Ischemia and hypoxia could induce neuronal injury, neurological dysfunction and severe long-term motor function injury. Histological staining and behavioural evaluations were performed to elucidate the pathological changes and neurobehavioural variation after ISO treatment. We found ISO administration significantly reduced the infarct volume of brain tissues and improved the autonomous activities of neonatal rats, ISO preconditioning significantly reduced neuronal apoptosis induced by HI, reduced cerebral infarction volume, improved histopathological damage of nerve cells, improved long-term cognitive function, and attenuated HI-induced Nissl total cells to reduce and reduce long-term spatial memory impairment caused by hypoxia-ischemia during the maturation of injured brain.

Conclusion

ISO preconditioning can protect the brain injury and promote the recovery of neurological function in neonatal rats with HIE, which may be through inhibiting the neuronal cell death in the cortex and hippocampus after HI.

1. Introduction

Hypoxic ischemic encephalopathy (HIE) is an important factor leading to neonatal death and neurodevelopmental disorders in clinical practice and is an irreversible cerebral ischemia-hypoxic injury caused by a variety of adverse perinatal factors, mainly include maternal eclampsia, umbilical cord entanglement, shoulder dystocia and placental abruption(Hu et al., 2017; Novak et al., 2018). It can lead to reduce or even interrupt cerebrovascular blood flow and is one of the most common causes in disabled children after the neonatal period. Neonatal brain injury can result in a range of permanent neurological sequelae, including epilepsy, cerebral palsy, motor and cognitive decline, attention-deficit hyperactivity disorder, and behavioral disability(Gulczyńska and Gadzinowski, 2012; Tagin et al., 2012; Odorcyk et al., 2017). Therefore, it imposes a huge mental and economic burden on families and has become one of the major medical problems worldwide. Studies have shown that about 0.2–0.4% of newborns may present with HIE (Kurinczuk et al., 2010). Newborns experience edema and necrosis of their nerve cells under ischemic and hypoxic conditions, and finally results in brain injury, which is bound to cause different degrees of cognitive and behavioral impairment in children if timely therapeutic measures are not taken (Dailey et al., 2013). HIE seriously affects the health and quality of life of patients, and causes a significant social and economic burden. Thus, the key to avoiding long-term neurological deficits induced by HIE is to alleviate the appearance of neuronal death and enhance synaptic plasticity in the acute phase. Herein, an unsolved medical problem needs to be studied to elucidate the mechanism and find effective neurotherapeutic goals(Wang et al., 2016). At present, mild hypothermia therapy is commonly used to treat HIE in clinical practice, but 40% − 50% of HIE severe children still undergo serious sequelae after treatment(Zhao et al., 2016). Therefore, subsequent rehabilitation is mostly adopted, but the treatment is time-consuming and the effect is uncertain, so it has become an urgent task to find a better treatment.

Isoflurane (ISO) is an inhalation anesthetic that inhibits inflammation, resists oxidative stress, and has some neuroprotective effects(Wang et al., 2014). After many years of clinical application, it has been found that it has the characteristics of reducing intracranial pressure, reducing cerebral oxygen consumption, inducing and maintaining balance, rapid recovery, and few side effects. At present, studies have shown that(Eger, 1981)low-dose ISO can reduce ischemic injury, and its mechanisms of action include: oxygen free radical injury, inflammatory response, activation of adenine receptor, activation of protein kinase C, and apoptosis and anti-apoptotic mechanisms. With the large use of isoflurane-based inhalation anesthetics in infant and neonatal surgery, there has been increasing concern about the cerebral protective effects produced by inhalation anesthetics. Compared with other conventional anesthetics, inhalational anesthetics are more commonly used because of their relatively safe route of administration and faster onset of action. Inhaled anesthetics, that is, anesthetic preconditioning, have been found to significantly reduce cerebral ischemia-reperfusion injury and have a protective effect on nerves in normal rats during cerebral ischemia(Low et al., 2016). Previous studies have shown that inhalation of appropriate anesthetic drugs has a certain preventive effect on reperfusion injury, and ISO anesthetic treatment has a certain protective effect on ischemia-reperfusion injury of important organs such as heart, liver, and kidney. ISO can reduce the compensatory function of its own brain function, lead to ischemic metabolism and pathological changes in the body. It is closely related to postoperative

cognitive dysfunction, and has the advantages of stable circulation and good muscle relaxation, which can effectively inhibit hippocampal neuronal cell apoptosis caused by cerebral ischemia-reperfusion injury, increase hypothalamic neuronal cell sodium and potassium currents, and help reduce cognitive impairment in aged rats(Duthie et al., 2019; Mashour, 2019). However, the role of ISO in protecting acute and long-term neurological deficits due to HIE is unclear and requires further investigation.

In this study, we established a neonatal rat model of hypoxia-ischemia, used ISO to precondition the model, and performed behavioral scoring and morphological staining on each group of animals to investigate the role of ISO preconditioning in the morphological and behavioral changes of hypoxic-ischemic brain injury in neonatal rats, which aimed to preliminarily explore its effect on long-term behavioral dysfunction in HIE rats and its possible mechanism and provide a new therapeutic strategy for clinical treatment of HIE.

2 Results

2.1 Status assessment

General manifestations of hypoxic-ischemic injury were occurred in neonatal SD rats at 5 to 20 min of hypoxia, including cyanosis, head shaking, shortness of breath, tail pinching, limb shaking, convulsions and other reactions; poor response, drowsiness, irregular breathing and other phenomena persisted until the end of hypoxia after 20 min.

2.2 HI induced cerebral damages in neonatal rats

Brain damages were caused indicated by anatomic appearance of brain tissues and TTC staining. The ipsilateral hemisphere of HI rat swelled obviously in comparison with that in sham group **(Figure. 1A)**. Meanwhile, significant infarct was revealed in the ipsilateral hemisphere by TTC staining, but no infarct was found in rats of the sham group **(Figure. 1B)**. These results elucidated the the successful establishment of HI models.

2.3 Pretreatment with isoflurane attenuated HI-induced neurological dysfunction in rats

2.3.1 Effects of Isoflurane Pretreatment on Spatial Learning, Memory and Cognitive Function in Rats After HI

The changes of learning and memory ability of rats in each group were observed by MWM test. The results showed that the mean escape latency of each group gradually decreased from day 1 to day 5. The escape latency was prolonged and the number of target crossing was reduced in the HI group. (Fig. 2A, B, $p = 0.013$, $p < 0.001$), but the escape latency was significantly decreased and the number of target crossing was increased after ISO pretreatment (Fig. 2A, B, $p = 0.042$, $p < 0.001$). The movement trajectory

of three groups were shown in the (Fig. 2C-E). The percentage of movement distance and residence time in the target quadrant were markedly reduced in the HI group (Fig. 2F, G, $p < 0.001$, $p = 0.002$), but got increased after ISO pretreatment (Fig. 2F, G, $p < 0.001$, $p = 0.005$).

The results of the Y-maze test showed that the longer walking distance, longer number of entries and duration in the food arm were displayed in rats with ISO pretreatment relative to rats in HI group (Fig. 3A-C, $p = 0.008$, $p = 0.003$, $p = 0.003$). In addition, the distance walked by the wrong arm, number of entries error arms and the residence time were increased in the HI group (Fig. 3G-I, $p < 0.001$, $p = 0.002$, $p < 0.001$), which were strikingly reduced in the Pretreatment group (Fig. 3G-I, $p = 0.003$, $p = 0.005$, $p < 0.001$). The walking trajectory maps of rats were showed in the (Figure 3D-F).

2.3.2 Effects of Isoflurane Pretreatment on Motor Function and Coordination in Rats After HI

To evaluate changes in motor function and coordination ability in rats after ISO pretreatment, we performed the rotarod test. In the rotarod test, the duration of rat stayed on the rotating rod was notably shorter after HI than that of sham group (Fig. 4, $p < 0.001$), while it was longer in rats underwent ISO pretreatment than that of HI injury (Fig. 4, $p = 0.016$). Results are expressed as mean ± SD. One-way analysis of variance (ANOVA) was used for multiple comparisons. If the data were normally distributed, Student-Newman-Keuls post-hoc test was performed. Otherwise, results were analyzed using Dunn's multiple comparison test. Escape latencies were analyzed using analysis of variance with repeated measures data followed by Bonferroni post-hoc tests. Relationship between morphology and behavior Pearson correlation analysis. Statistical analysis was performed using SPSS 21.0 software and histograms were plotted by GraphPad Prism 8 software. $P < 0.05$ was considered statistically significant.

2.4 ISO ameliorated the acute cerebral injury induced by HI in neonatal rats

In order to demonstrate the effect of HI on neuronal survival in the brain, Nissl staining was performed 1 day after modeling to analyze neuronal cell survival in this model. Results of Nissl staining exhibited that in the sham group, the cells of each layer were neatly arranged with abundant Nissl bodies, clearly visible oval nucleoli. Cells in HI group demonstrated the disordered cells arrangement, neuronal necrosis and reduced Nissl bodies. But in Pretreatment group, the number of necrotic neurons decreased, and Nissl bodies were significantly increased (Fig. 5A). Compared with the sham group, the total neurons in the cortex (Fig. 5B, $p < 0.001$) and the hippocampus (Fig. 5C, $p < 0.001$) were significantly decreased in the HI group, which was decreased after ISO pretreatment (Fig. 5B, C, $p < 0.001$, $p < 0.001$). Moreover, there were more total neurons in the CA1, CA2, CA3, and DG regions of the hippocampus and fewer dark neurons in the pretreatment group compared to the HI group (Fig. 5D, $p < 0.01$).

As shown by HE staining, the right brain structure of the sham rats was intact, and the various nerve cells in normal shape have complete structure. The nucleus is located in the centre of the cell body, with clear

nuclear membrane and obvious nucleoli. However, the brain tissues in the HI group were denatured and necrotic, where cortical cells were disordered and fragmented. Many vacuoles were formed. Neuronal and cellular structures disappeared, and a large number of inflammatory cells infiltrated. However, after ISO pretreatment, the disorder of cell arrangement in the right cerebral cortex was obviously improved, and the morphology of neurons was close to normal ones in sham group (Fig. 6).

2.5 ISO treatment ameliorated cerebral pathological changes in neonatal HI rats

Nissl staining was used to detect the survival of neurons, and as a result, Nissl stained neurons were detected in both cortical and hippocampal regions 42 d after HI. In the sham group, the neurons had intact morphological structure, large, neatly arranged cell bodies, uniform staining, and abundant cytoplasm and Nissl bodies; however, in the HI group, the neurons were irregularly arranged and showed extensive neuronal damage, such as pyknosis, increased space, decreased volume, dark blue nuclei, interstitial swelling, neuronal structure, and disappearance of Nissl bodies (Fig. 7A). Similar to the 1d results, the number of Total neurons decreased significantly after HI, and the number of Dark neurons increased compared with the sham group, and the difference was statistically significant (Fig. 7B, $p < 0.001$; Fig. 7C, $p < 0.001$). Compared with the HI group, the Pretreatment group had an increased number of total neurons in the CA1, CA2, CA3, DG of the hippocampus regions and cortical regions (Fig. 7D, $p = 0.001$, $p = 0.011$, $p = 0.005$, $p < 0.003$) and a decreased number of dark neurons (Fig. 7D, $p = 0.001$, $p = 0.01$, $p = 0.019$, $p = 0.015$).

HE staining was used to observe the morphological changes of brain tissue at 42 days, and the hippocampal tissue morphology of rats in the sham group was normal, the space around the cells and microvessels was normal, the nuclei were large and round, and the nuclear chromatin was uniform and clear; compared with the sham group, more cell cavities appeared in the cortex, CA1, CA2, CA3 and DG regions of the hippocampus after HI, the nuclei were pyknotic, irregularly arranged and the nuclei pressed to one side of the neuronal cells, the brain swelling was more severe, the chromatin of gliotic nuclei was blurred, the space around the cells and microvessels was significantly widened, the tissue space was significantly swollen, the nuclei were pyknotic, densely stained or even ruptured. However, after treatment with ISO, the cell morphology in the cortical hippocampus was more complete than that in the HI group, with less nucleolus reduction **(Figure.8).** These suggested that ISO could alleviate cell damage in neonatal HI rats.

2.6 Correlation Analysis between Behavior and Morphology in HIE Rats

To investigate whether there was a correlation between the impairment of morphology and behavioral performance we used Pearson's correlation analysis to explore the correlation analysis between behavior and morphology in HIE rats. We used the percentage of Dark neurons in total neurons in morphology and

various parameters of MWM, Y-maze, and rotarod for analysis. The results showed that there was a significant negative correlation between morphology and various indicators of water maze, rotarod, and Y-maze (number and duration of food arm entries), with correlation coefficients ranging from-0.8694 to-0.6145, and the difference was statistically significant (Fig. 9A-F, $p < 0.01$). There was a significant positive correlation with the number, duration, and distance of Y-maze error arm entries, with correlation coefficients ranging from 0.8264 to 0.7512, and the difference was statistically significant (Fig. 9G-I, $p < 0.01$). However, the correlation of food arm distance was poor, with a correlation coefficient of 0.2123, (Fig. 9F, $p < 0.01$).

3 Discussion

In this study, we found that inhalation of 2% ISO for 1 hour before and after hypoxic-ischemic brain damage in neonatal rats significantly promoted neuronal regeneration, inhibited neuronal apoptosis, and improved motor and cognitive function, and ISO pretreatment inhibited neuronal cell death in the cerebral cortex, CA1, CA2, CA3, and DG of neonatal rats; that is, it improved acute and long-term neurological deficits induced by hypoxic-ischemic brain damage in neonatal rats.

Previous studies have successfully established neonatal HI models using Rice-Vannucci method and confirmed the degree of neurological and motor impairment of HI rats. In this study, we applied a lot of behavioral experiments to determine the acute as well as long-term neurological defects after HI injury. Among them, WMW and Y-maze were usually carried out to investigate the learning and memory abilities(Potschka et al., 2000; Meirsman et al., 2016), and Rotarod test were used to observe the exercise and coordination function of rats(Balduini et al., 2000; Chu et al., 2004). Through these tests, we found that the Morris water maze and Y-maze test were strongly corresponded regarding the activities of neurological improvement. Behavioral evaluation can be used to assess long-term behavioral changes in HIE rats. Behavioral assessment of rats 1 month after HI injury further determined the efficacy of ISO for long-term neuroprotection. The experimental results showed that ISO reduced the severity of long-term neurological injury, improved long-term spatial learning and memory abilities, and increased motor coordination in HI rats. the HI group showed severe learning and memory impairment, and the littermates in the Pretreatment group were not significantly different from those in the sham group, show that ISO pretreatment can protect neurocognitive function. Our results are consistent with the study by Shao et al. (Shao et al., 2006). Animals in the HI group had more pronounced pathological damage to brain morphology, and these findings confirm previous studies showing a correlation between learning impairment and ipsilateral hemispheric and hippocampal tissue loss(Ten et al., 2004; Cengiz et al., 2011).

An increasing number of studies have shown that HI causes irreversible brain damage to the developing brain of newborns, resulting in long-term neurological deficits. Microvascular responses and blood-brain barrier damage in neonatal HI models lead to brain injury(Wang et al., 2016). HE and Nissl staining can usually calculate the degree of injury and the number of necrotic neurons. The hippocampus and cortex are very sensitive to ischemia-hypoxia injury(Li et al., 2017a), so in this study, the above regions were selected to observe the morphological changes of neurons. At 24 h after HI, the neurons of hippocampal

CA1□CA3 and cortex in the HI group showed significant morphological damage, with loss of neurons and Nissl bodies, pyknotic nuclei, and vacuolization. The results of Nissl staining clearly showed that HIE induced extensive apoptosis in the ipsilateral hemisphere, which was effectively prevented by conditioning after ISO preconditioning, and the results of Galle et al were consistent(Galle and Jones, 2013), further confirming that ISO preconditioning has a neuroprotective effect. Pathologically, ISO pretreatment alleviated neuronal edema and necrosis, irregularly arranged Nissl bodies, incomplete cellularity, and inflammatory cell infiltration occurring in the cerebral cortex. The number of Nissl positive cells in the cortex and hippocampus increased after ISO pretreatment, indicating that ISO inhibits neuronal cell death in HI rats. Bauer, T.M.et al.(Galle and Jones, 2013) it was confirmed that ISO postconditioning had a protective effect on hypoxic-ischemic brain damage in neonatal rats, and this protective effect may be related to the inhibition of the opening of mitochondrial permeability transition pore (mPTP).Opening of mPTP can lead to impaired energy synthesis and cellular oxidative response, triggering a cascade, resulting in decreased ATP levels, while the increase in intracellular $Ca2^{+}$ concentration is closely related to ATP levels(Galle and Jones, 2013; Bauer and Murphy, 2020).It is generally accepted that the elimination ability is reduced by massive release of glutamate during ischemia and hypoxia, the extracellular glutamate concentration is greatly increased to toxic levels, glutamate receptors are hyperactivated, and massive influx of $Ca2^{+}$ leads to cell swelling and apoptosis, and this process is mainly mediated by AMPA receptors(Henley et al., 2011). It has been documented that administration of AMPA receptor antagonists to neonatal rats with hypoxic-ischemic brain damage alone can reduce the inflammatory response and peroxide levels in brain cells and reduce the degree of brain injury(Bauer and Murphy, 2020). The excitatory neurotransmitter AMPA, on the other hand, activates AMPA receptors and causes changes in their configuration resulting in damaging effects, and it has also been shown to cause brain tissue damage. The results of this experiment showed that ISO pretreatment in neonatal rats with hypoxic-ischemic brain damage significantly improved the degree of brain injury, and the number of normal neurons in the hippocampus of the right brain was significantly increased at 1 d of ischemia and hypoxia.

Through correlation analysis between behavior and morphology, we found that there was a strong correspondence between WMW and Y-maze had a strong corresponding relationship in the improvement of nerve activity, especially a significant negative correlation between WMW and Rotated various indicators. Thus, the behavioral difference between WMW and Y-maze can be used as a behavioral assessment reference for brain injury. These results all reveal that ISO preconditioning can improve spatial learning and memory abilities, as well as long-term motor function with positive effects.

ISO is an inhalation anesthetic with certain analgesic and muscle relaxant effects. There is no contraindication for its use. It is applicable to various types of intraoperative anesthesia. It has a close relationship with the biological behavior of malignant tumor histiocytes such as colorectal cancer, prostate cancer, and glioma(Hu et al., 2018; Liu et al., 2019).A large number of studies have reported that low-dose ISO has antioxidant, anti-apoptotic and immunomodulatory effects, and has a good protective effect on various acute central nervous system injuries such as cerebral ischemia-hypoxia injury and

reperfusion injury(Zimin et al., 2018).In addition, some studies have confirmed that ISO can regulate the activation of NF-KB signaling pathway(Li et al., 2008; Yao et al., 2020), and ISO or multiple treatments during development can affect spatial cognitive behavior in rats as adults(Katiyar et al., 2018). Previous studies(Li et al., 2017b; Agnic et al., 2018) have shown that ISO may contribute to postoperative cognitive dysfunction in elderly patients by eliciting neuroinflammation, disrupting choline function, and synaptic plasticity. It can induce postoperative cognitive dysfunction and promote neuronal apoptosis. Recent studies(Yang et al., 2020)have shown that ISO can alleviate the inflammatory factor analysis and the degree of lipid peroxidation in rats with cerebral ischemia/reperfusion injury through TGF-beta1/Smad2/3 Signaling Pathway, reduce the hydrolytic activity of matrix metalloproteinases in brain tissue, reduce tight junction protein loss, and improve cerebral ischemia-reperfusion injury in rats. The in vitro studies(Yan et al., 2016), demonstrated that ISO preconditioning reduced the release of OGD-induced lactate dehydrogenase (LDH) and enhanced the OGD-inhibited cell viability. It has also been observed that the hypoxia inducible factor-1α (HIF-1α) was increased under ISO preconditioning. In fact, these results thus suggest that the ISO preconditioning may provide potential neuroprotection against Cerebral ischemic/reperfusion injury via up-regulating the HIF-1α expression through the Akt/mTOR/s6K activation. McAuliffe et al. (McAuliffe et al., 2007)studied the long-term effects of delayed preconditioning with Iso, hypoxia, or room air on motor and cognitive function in mice subjected to hypoxia-ischemia for 65 minutes at postnatal day 10. Delayed preconditioning of Iso and hypoxia in neonatal mice improved learning and memory with functional neuroprotection. Xiong et al. (Xiong et al., 2003) study demonstrated that repeated Iso anesthesia induces ischemic tolerance in rats in a dose-response manner. GLB, an adenosine triphosphate-regulated potassium channel blocker, abolished the tolerance induced by Iso. Brief isoflurane anesthesia induces ischemic tolerance in the brain. The effect was found to be dose dependent in a rat focal cerebral ischemia model. Ischemic tolerance induced by isoflurane preconditioning is dependent on activation of adenosine triphosphate-regulated potassium channels. The effects of ISO on the nervous system are wide-ranging and complex, so active studies of the mechanism of action of ISO on the nervous system are helpful to better understand the effects.

HIE is a common neonatal disease in clinical practice at present, and the pathogenesis includes mitochondrial damage, oxidative stress, neurotoxicity of excitatory amino acids, and inflammatory immune response due to the results of a combination of cellular and molecular mechanisms. Its occurrence is mainly related to perinatal asphyxia and plays an indispensable role in perinatal neurological diseases, which can cause brain tissue hypoxia, interruption or reduction of cerebral blood flow, brain injury in newborns, neurological injury, and severe death in children(Schump, 2018; Narayanamurthy et al., 2021).There is increasing evidence that HI causes irreversible brain damage to the developing brain, leading to long-term neurological deficits. The incidence of neurological sequelae is relatively high, resulting in an increased incidence of disability, and the earlier this type of disease, the better the therapeutic effect. At present, mild hypothermia therapy is often used to treat moderate and severe full-term HIE children in clinical practice, which has a regulatory effect on the body's cerebral blood flow and can reduce neuronal apoptosis and relieve neurological symptoms such as disturbance of consciousness and floppy limbs in children(Brekke et al., 2014).It is undeniable that hypothermia

treatment is recognized as an effective treatment for HIE(Saw et al., 2019; Finder et al., 2020).However, its clinical application is limited due to the short treatment window and other reasons. In addition, the pathogenesis and clinical characteristics of HIE are complex. Current studies have shown that drugs combined with hypothermia are more effective in the treatment of HIE(Lin et al., 2014; Landucci et al., 2018; Barata et al., 2019). In order to make the neuroprotective effect of HIE more clinically applicable, combined hypothermia treatment needs to be further considered and explored to achieve more targets and enhance neuroprotection. There is a lack of drugs for the treatment of HIE in clinical practice, and it is still urgent to find safe and effective drugs from natural products.

The main finding of this study was that ISO pretreatment not only protected neonatal rats with HIE from brain injury, but also promoted their neurological recovery but also improved their learning and memory, possibly by inhibiting cell death in the cortex and hippocampus after HI. After ISO preconditioning, motor function will be restored to reduce brain injury and improve neurological function provides a new idea. It is worth noting that the specific mechanism of the protective effect of ISO pretreatment has not been fully clarified, and in the next step we will further study it in depth.

4 Materials And Methods

4.1 Experimental Animals and Groups

The animal protocol of this study was approved by the Animal Protection and Welfare Committee of Kunming Medical University (Ethics number: Kmmu 20220748), and pregnant female SD rats used in the study were purchased from the Laboratory Animal Center of Kunming Medical University and caged individually. After birth, pups were housed next to dams on a 12-hour (h) light cycle with ad libitum access to a diet. Subsequently, 7 d rat pups (weighing 12–15 g) were used for subsequent studies. Thirty-nine experimental animals were randomly divided into sham operation group (sham group), ischemia-hypoxia group (HI group), and ISO preconditioning group (Pretreatment group) according to the random number table, with 13 animals in each group. All experimental procedures were performed in accordance with the procedures approved by the Animal Protection Committee of Kunming Medical University. The feeding and care of laboratory animals followed the regulations of the Chinese Committee for the Protection and Ethics of Laboratory Animals, as well as the regulations of the National Institute for Ethical Guidelines for Laboratory Animals in Health and Hygiene.

4.2 Main reagents and instruments

Isoflurane was purchased from Shenzhen Reward Life Science & Technology Co., Ltd., batch number: 81122; monopolar microsurgical coagulator was purchased from Wuhan Chunguang Medical Cosmetic Instrument Co., Ltd., model: B; ZKY-4F oxygen concentration detector was purchased from Hangzhou Epp Instrument and Equipment Co., Ltd., model: AP2018100802; Morris water maze and Y-maze were purchased from Shanghai Xinruan Technology Co., Ltd.; hematoxylin-eosin staining solution was purchased from Beijing Solaibao Biotechnology Co., Ltd., batch number: C0117; Nissl staining solution

was purchased from Shanghai Biyuntian Biotechnology Co., Ltd., batch number: 202112; the manufacturer of whole section scanner was Dangel with model number 2020066771.

4.3 Establishment of hypoxic-ischemic (HI) model

7 d neonatal rats were anesthetized with 5% ISO inhalation and 3% maintenance anesthesia. The rats were fixed in supine position on the operating table and the neck was disinfected with iodophor. 0.5 cm incision was opened with surgical scissors in the median sagittal line of the neck of young rats. The cervical tissue was separated layer by layer with forceps to expose the right common carotid artery (LCCA). After the LCCA was separated with microforceps, coagulated with a monopolar microsurgical coagulator (Wuhan Medical Cosmetic Instrument Co., Ltd. Model: CHR-3). Care was taken not to pull the vessels and touch the vagus nerve. The subcutaneous tissue and skin were sutured. Finally, the rats were disinfected with local iodophor and placed back to the dams. After 1 h of recovery, the rats were placed in a closed hypoxia box for 2 h. The box was continuously filled with a mixture containing (6.8–7.4) % oxygen + (93.2–92.6%) nitrogen, with a gas flow rate of 1.5 L/min, a temperature maintained at (33 ± 1) ℃, and a humidity of 50% -70% to achieve the purpose of hypoxia. The animals in the pretreatment group were modeled with 2% ISO inhalation for 1 h before the ischemia and hypoxia, and the animals in the sham group were only anesthetized to expose the LCCA without electrocoagulation or hypoxia treatment, and the vital signs of all rats needed to be closely monitored after modeling.

4.4 Behavioral Testing

Behavioral analysis was used to assess the functional status of the experimental animals and the nervous system. Water maze test(Yang et al., 2017)and Y-maze(Kraeuter et al., 2019)were used to assess the neurobehavioral function of rats, which were mainly related to spatial memory, learning and other abilities. The rotarod test (Hamm et al., 1994) was performed to assess the motor function of rats, and severe dyskinesia or poor coordination affected the animal's ability to remain on the rotating rod when speed increased.

4.4.1 Morris Water Maze (MWM)

The MWM test was performed at model 30th day, which consisted of two parts. The spatial learning ability test was performed four times a day from 9:00 am to 12:00 am for 5 days, and each rat needed to be tested in different quadrants. The time of platform discovery was observed and analyzed. If it was not found within 90 seconds (s), it was necessary to guide it to the platform and stay for 20 s. After test, the rat was removed from the water, wiped the water on the rat with a cotton cloth, and dried it with a radiator. Parameters such as water entry position, swimming speed, search target time, and movement trajectory were collected and analyzed by SuperMaze software. In the spatial memory test, the platform was withdrawn and each rat was placed in the same selected quadrant (the quadrant opposite the original hidden platform) on the 6th day. The tracking software recorded the time spent in the probed quadrant and the swimming path for 1 min. Residence time was used to measure spatial memory. During the experiment, quiet and constant light was maintained and the placement of the objects also remained

unchanged. The time the rat spent in the target quadrant and the number of entries into the target quadrant were recorded as a measure of the rats' spatial memory ability.

4.4.2 Y-maze test

The Y-maze test was performed after the end of the MWM and the system consisted of three parts: the starting arm, the wrong arm, and the food arm. There were two main stages. The first stage was the training period. The rats were fasted for 1 ~ 2 times, and their body weight decreased to 85% of the original body weight. The rats were placed in the starting arm of the instrument, allowed to move in the maze driven by food, and each rat's movement was observed and recorded. The experiment was 5 min each time, 10 min per day for 3 consecutive days. The second session was a test session in which the wrong arm partition was withdrawn and the rat was placed by the starting arm and allowed to move freely in three arms for 5 min. The SuperMaze V2.0 system was videotaped to record the number of times the rat entered each arm and the dwell time within 5 min.

4.4.3 Rotarod test

The rotarod test was used to assess motor coordination and gross motor function in rats. The rats were underwent adaptive training three days before the experiment, placed on a rotarod fatigue instrument (10 rmp/min) for training three times a day for 10 min. On the third day of testing, they were rotated at a uniform speed of 30 rmp/min, and before the second test, the rats were rested for 30 min for three tests. The mean value of the three times of rat dropping was recorded for inclusion in the score. Animals with severe dyskinesia or poor coordination fall during rotarod rotarod movement, and the longer time stayed on the fatigue instrument, the better its coordination.

4.5 Morphological Staining

4.5.1 Tissues Harvest

After all behavioral tests were completed on 1 and 42 days after modeling, anesthesia was induced with 5% ISO inhalation, anesthesia was maintained with 3%, the rats were fixed in the supine position, the abdominal skin was lifted, the abdominal cavity was opened at the xiphoid process position, the thoracic cavity was cut along both costal arches, the xiphoid process was clamped with hemostatic forceps to turn upwards, and the thoracic cavity was exposed; the connective tissue around the heart was cut to dissect the pericardium, the heart was freed, the heart and ascending aorta were fully exposed, a perfusion needle was inserted from the apical site, an extension tube was connected deep to the aortic root, the needle was fixed with an arterial clamp, and the right atrial appendage was cut. About 50 mL of 0.9% sodium chloride injection was rapidly perfused, and after the fluid flowing from the right atrial appendage was clarified, about 50 mL of 4% paraformaldehyde was continued to be slowly perfused until showing extension and convulsion of the limbs, stiff tail, and generalized rigidity in rats. The rats were fixed prone, the skin of the head was cut open, the skull was carefully dissected by decapitation, the brain tissue was removed, placed in 4% paraformaldehyde solution, and fixed for 24 h for subsequent staining.

4.5.2 Preparation of Paraffin Sections

First, the brain tissue was trimmed anteriorly from the herringbone suture into a coronal section of 4 mm, washed with running water in the cassette for 6 h, followed by dehydration with 70%, 80%, 90%, and 95% alcohol, as well as 100% alcohol I and 100% alcohol II solutions for 1 h each, and then placed in xylene I and xylene II solutions for 30 min each to make the tissue transparent. The tissues were embedded in a paraffin embedding machine (Leica model: EG1150H), and then serially sectioned into 4 μm sections using a paraffin microtome (Leica model: RM2235). Sections were cleared and hydrated through xylene and graded alcohols for subsequent staining.

4.5.3 Triphenyl Tetrazolium Chloride (TTC) staining

At 24 h and 7 d after HI surgery, rats were anesthetized with 2.5% isoflurane and euthanized. Brain tissues were rapidly exposed, harvested, and photographed for anatomic appearance. Frozen brain tissues were sectioned into 2 mm coronal sections (total 5 slices) in a rat brain matrix (Seino Co., Ltd. Beijing, China) befor being immersed in 2% solution of 2, 3, 5 triphenyl tetrazolium chloride (Sigma Co., St Louis, MO, USA) in a dark incubator at 37 ℃ for 10 min. Subsequently, fixation with 4% paraformaldehyde was followed, and the infarct area was tracked and analyzed by Image J Software (V1.8.0.112; National Institutes of Health, Bethesda, MD, USA).

4.5.4 HE staining

The treated paraffin sections were dropped with hematoxylin staining solution for about 3 min, rinsed with tap water for 5 min, and then the sections were differentiated by dropping 1% hydrochloric acid ethanol solution to fade for about 30 s. The sections were seen to turn red and light in color. The sections were then returned to blue in running tap water for approximately 5 min. Eosin staining was performed for 1 min, followed by xylene clearing after dehydration from low to high gradients of alcohol. Sections were mounted by neutral gum and observed microscopically.

4.5.5 Nissl staining

The prepared slides were dipped in Nissl staining solution at room temperature for 10 min. The staining solution was decanted, and the tissue was placed in 70% alcohol for differentiation, rapidly dehydrated with absolute ethanol, cleared with xylene, and mounted with neutral gum. Three sections were randomly selected from each rat and scanned by a digital section scanner (Tangel model: 2020066771), and the percentage of neuron-positive cells with positive Nissl staining in the hippocampus (CA1, CA2, CA3, and DG regions) and cortex to the total number of cells was analyzed with Image J software, and five fields were randomly selected from each section to count the number of nerve cells with Image J.

4.6 Statistical Analysis

The results were expressed as mean ± SD. One-way analysis of variance (ANOVA) was used for multiple comparisons between different groups. If the data were normally distributed, Student-Newman-Keuls post-hoc test was performed. If not, Dunn's Multiple Comparison test was used to analyze the results.

Escape latency was analyzed using analysis of variance using repeated measures data followed by Bonferroni post-hoc test. Relationship between morphology and behavior Pearson correlation analysis. SPSS 21.0 software was used for statistical analysis, and GraphPad Prism 8 software was used to draw histograms. $p < 0.05$ was considered statistically significant.

Abbreviations

HI, hypoxic-ischemic; HIE, Hypoxic-ischemic encephalopathy; MWM, Morris water maze;; SD, Sprague Dawley; TTC, 2,3,4-tiphenyl tetrazolium chloride;; d, day; mon, month; h, hour; min, minute; s, second

Declarations

Conflict of Interest

The authors declare that the research was conducted in the absence of any commercial or financial relationships that could be construed as a potential conflict of interest.

Author Contributions

THW and LLX participated in the design, review of this study. YBW, TBC and XF carried out the experiment. YBW, HFLR and HSZ interpreted the data and arranged

figures. YBW and QXX wrote and revised the manuscript. TBC and HSZ helped to finalize the manuscript. All authors have read and approved the final version of the manuscript.

Funding

This study was supported by Project of Guizhou Health Committee (No. gzwjkj2020-1-014) and Doctoral Start-up Fund of Affiliated Hospital of Zunyi Medical University (No.201903).

Acknowledgments

We are grateful to Kunming Medical University (Yunnan, China) for providing animals. We would like to thank Prof. Jia Liu from Animal Zoology Department, Kunming Medical University for their technical support.

References

1. Agnic, I., Filipovic, N., Vukojevic, K., Saraga-Babic, M., and Grkovic, I. (2018). Isoflurane post-conditioning influences myocardial infarct healing in rats. *Biotech Histochem* 93(5)**,** 354-363. doi: 10.1080/10520295.2018.1443507.
2. Balduini, W., De Angelis, V., Mazzoni, E., and Cimino, M. (2000). Long-lasting behavioral alterations following a hypoxic/ischemic brain injury in neonatal rats. *Brain Res* 859(2)**,** 318-325. doi:

10.1016/s0006-8993(00)01997-1.

3. Barata, L., Arruza, L., Rodríguez, M.J., Aleo, E., Vierge, E., Criado, E., et al. (2019). Neuroprotection by cannabidiol and hypothermia in a piglet model of newborn hypoxic-ischemic brain damage. *Neuropharmacology* 146**,** 1-11. doi: 10.1016/j.neuropharm.2018.11.020.
4. Bauer, T.M., and Murphy, E. (2020). Role of Mitochondrial Calcium and the Permeability Transition Pore in Regulating Cell Death. *Circ Res* 126(2)**,** 280-293. doi: 10.1161/circresaha.119.316306.
5. Brekke, E.M., Morken, T.S., Widerøe, M., Håberg, A.K., Brubakk, A.M., and Sonnewald, U. (2014). The pentose phosphate pathway and pyruvate carboxylation after neonatal hypoxic-ischemic brain injury. *J Cereb Blood Flow Metab* 34(4)**,** 724-734. doi: 10.1038/jcbfm.2014.8.
6. Cengiz, P., Uluc, K., Kendigelen, P., Akture, E., Hutchinson, E., Song, C., et al. (2011). Chronic neurological deficits in mice after perinatal hypoxia and ischemia correlate with hemispheric tissue loss and white matter injury detected by MRI. *Dev Neurosci* 33(3-4)**,** 270-279. doi: 10.1159/000328430.
7. Chu, K., Jeong, S.W., Jung, K.H., Han, S.Y., Lee, S.T., Kim, M., et al. (2004). Celecoxib induces functional recovery after intracerebral hemorrhage with reduction of brain edema and perihematomal cell death. *J Cereb Blood Flow Metab* 24(8)**,** 926-933. doi: 10.1097/01.Wcb.0000130866.25040.7d.
8. Dailey, T., Mosley, Y., Pabon, M., Acosta, S., Tajiri, N., van Loveren, H., et al. (2013). Advancing critical care medicine with stem cell therapy and hypothermia for cerebral palsy. *Neuroreport* 24(18)**,** 1067-1071. doi: 10.1097/wnr.0000000000000062.
9. Duthie, A., van Aalten, L., MacDonald, C., McNeilly, A., Gallagher, J., Geddes, J., et al. (2019). Recruitment, Retainment, and Biomarkers of Response; A Pilot Trial of Lithium in Humans With Mild Cognitive Impairment. *Front Mol Neurosci* 12**,** 163. doi: 10.3389/fnmol.2019.00163.
10. Eger, E.I., 2nd (1981). Isoflurane: a review. *Anesthesiology* 55(5)**,** 559-576. doi: 10.1097/00000542-198111000-00014.
11. Finder, M., Boylan, G.B., Twomey, D., Ahearne, C., Murray, D.M., and Hallberg, B. (2020). Two-Year Neurodevelopmental Outcomes After Mild Hypoxic Ischemic Encephalopathy in the Era of Therapeutic Hypothermia. *JAMA Pediatr* 174(1)**,** 48-55. doi: 10.1001/jamapediatrics.2019.4011.
12. Galle, A.A., and Jones, N.M. (2013). The neuroprotective actions of hypoxic preconditioning and postconditioning in a neonatal rat model of hypoxic-ischemic brain injury. *Brain Res* 1498**,** 1-8. doi: 10.1016/j.brainres.2012.12.026.
13. Gulczyńska, E., and Gadzinowski, J. (2012). [Therapeutic hypothermia for neonatal hypoxic-ischemic encephalopathy]. *Ginekol Pol* 83(3)**,** 214-218.
14. Hamm, R.J., Pike, B.R., O'Dell, D.M., Lyeth, B.G., and Jenkins, L.W. (1994). The rotarod test: an evaluation of its effectiveness in assessing motor deficits following traumatic brain injury. *J Neurotrauma* 11(2)**,** 187-196. doi: 10.1089/neu.1994.11.187.
15. Henley, J.M., Barker, E.A., and Glebov, O.O. (2011). Routes, destinations and delays: recent advances in AMPA receptor trafficking. *Trends Neurosci* 34(5)**,** 258-268. doi: 10.1016/j.tins.2011.02.004.

16. Hu, F., Li, T., Gong, H., Chen, Z., Jin, Y., Xu, G., et al. (2017). Bisphenol A Impairs Synaptic Plasticity by Both Pre- and Postsynaptic Mechanisms. *Adv Sci (Weinh)* 4(8), 1600493. doi: 10.1002/advs.201600493.
17. Hu, J., Hu, J., Jiao, H., and Li, Q. (2018). Anesthetic effects of isoflurane and the molecular mechanism underlying isoflurane-inhibited aggressiveness of hepatic carcinoma. *Mol Med Rep* 18(1), 184-192. doi: 10.3892/mmr.2018.8945.
18. Katiyar, K.S., Winter, C.C., Gordián-Vélez, W.J., O'Donnell, J.C., Song, Y.J., Hernandez, N.S., et al. (2018). Three-dimensional Tissue Engineered Aligned Astrocyte Networks to Recapitulate Developmental Mechanisms and Facilitate Nervous System Regeneration. *J Vis Exp* (131). doi: 10.3791/55848.
19. Kraeuter, A.K., Guest, P.C., and Sarnyai, Z. (2019). The Y-Maze for Assessment of Spatial Working and Reference Memory in Mice. *Methods Mol Biol* 1916, 105-111. doi: 10.1007/978-1-4939-8994-2_10.
20. Kurinczuk, J.J., White-Koning, M., and Badawi, N. (2010). Epidemiology of neonatal encephalopathy and hypoxic-ischaemic encephalopathy. *Early Hum Dev* 86(6), 329-338. doi: 10.1016/j.earlhumdev.2010.05.010.
21. Landucci, E., Filippi, L., Gerace, E., Catarzi, S., Guerrini, R., and Pellegrini-Giampietro, D.E. (2018). Neuroprotective effects of topiramate and memantine in combination with hypothermia in hypoxic-ischemic brain injury in vitro and in vivo. *Neurosci Lett* 668, 103-107. doi: 10.1016/j.neulet.2018.01.023.
22. Li, B., Concepcion, K., Meng, X., and Zhang, L. (2017a). Brain-immune interactions in perinatal hypoxic-ischemic brain injury. *Prog Neurobiol* 159, 50-68. doi: 10.1016/j.pneurobio.2017.10.006.
23. Li, Y., Zhang, X., Zhu, B., and Xue, Z. (2008). Desflurane preconditioning inhibits endothelial nuclear factor-kappa-B activation by targeting the proximal end of tumor necrosis factor-alpha signaling. *Anesth Analg* 106(5), 1473-1479, table of contents. doi: 10.1213/ane.0b013e318168b3f2.
24. Li, Z., Ni, C., Xia, C., Jaw, J., Wang, Y., Cao, Y., et al. (2017b). Calcineurin/nuclear factor-κB signaling mediates isoflurane-induced hippocampal neuroinflammation and subsequent cognitive impairment in aged rats. *Mol Med Rep* 15(1), 201-209. doi: 10.3892/mmr.2016.5967.
25. Lin, E.P., Miles, L., Hughes, E.A., McCann, J.C., Vorhees, C.V., McAuliffe, J.J., et al. (2014). A combination of mild hypothermia and sevoflurane affords long-term protection in a modified neonatal mouse model of cerebral hypoxia-ischemia. *Anesth Analg* 119(5), 1158-1173. doi: 10.1213/ane.0000000000000262.
26. Liu, R., Li, X., and Zhao, G. (2019). Beclin1-mediated ferroptosis activation is associated with isoflurane-induced toxicity in SH-SY5Y neuroblastoma cells. *Acta Biochim Biophys Sin (Shanghai)* 51(11), 1134-1141. doi: 10.1093/abbs/gmz104.
27. Low, L.A., Bauer, L.C., and Klaunberg, B.A. (2016). Comparing the Effects of Isoflurane and Alpha Chloralose upon Mouse Physiology. *PLoS One* 11(5), e0154936. doi: 10.1371/journal.pone.0154936.
28. Mashour, G.A. (2019). Role of cortical feedback signalling in consciousness and anaesthetic-induced unconsciousness. *Br J Anaesth* 123(4), 404-405. doi: 10.1016/j.bja.2019.07.001.

29. McAuliffe, J.J., Joseph, B., and Vorhees, C.V. (2007). Isoflurane-delayed preconditioning reduces immediate mortality and improves striatal function in adult mice after neonatal hypoxia-ischemia. *Anesth Analg* 104(5), 1066-1077, tables of contents. doi: 10.1213/01.ane.0000260321.62377.74.

30. Meirsman, A.C., Le Merrer, J., Pellissier, L.P., Diaz, J., Clesse, D., Kieffer, B.L., et al. (2016). Mice Lacking GPR88 Show Motor Deficit, Improved Spatial Learning, and Low Anxiety Reversed by Delta Opioid Antagonist. *Biol Psychiatry* 79(11), 917-927. doi: 10.1016/j.biopsych.2015.05.020.

31. Narayanamurthy, R., Yang, J.J., Yager, J.Y., and Unsworth, L.D. (2021). Drug delivery platforms for neonatal brain injury. *J Control Release* 330, 765-787. doi: 10.1016/j.jconrel.2020.12.056.

32. Novak, C.M., Ozen, M., and Burd, I. (2018). Perinatal Brain Injury: Mechanisms, Prevention, and Outcomes. *Clin Perinatol* 45(2), 357-375. doi: 10.1016/j.clp.2018.01.015.

33. Odorcyk, F.K., Sanches, E.F., Nicola, F.C., Moraes, J., Pettenuzzo, L.F., Kolling, J., et al. (2017). Administration of Huperzia quadrifariata Extract, a Cholinesterase Inhibitory Alkaloid Mixture, has Neuroprotective Effects in a Rat Model of Cerebral Hypoxia-Ischemia. *Neurochem Res* 42(2), 552-562. doi: 10.1007/s11064-016-2107-6.

34. Potschka, H., Friderichs, E., and Löscher, W. (2000). Anticonvulsant and proconvulsant effects of tramadol, its enantiomers and its M1 metabolite in the rat kindling model of epilepsy. *Br J Pharmacol* 131(2), 203-212. doi: 10.1038/sj.bjp.0703562.

35. Saw, C.L., Rakshasbhuvankar, A., Rao, S., Bulsara, M., and Patole, S. (2019). Current Practice of Therapeutic Hypothermia for Mild Hypoxic Ischemic Encephalopathy. *J Child Neurol* 34(7), 402-409. doi: 10.1177/0883073819828625.

36. Schump, E.A. (2018). Neonatal Encephalopathy: Current Management and Future Trends. *Crit Care Nurs Clin North Am* 30(4), 509-521. doi: 10.1016/j.cnc.2018.07.007.

37. Shao, G., Zhang, R., Wang, Z.L., Gao, C.Y., Huo, X., and Lu, G.W. (2006). Hypoxic preconditioning improves spatial cognitive ability in mice. *Neurosignals* 15(6), 314-321. doi: 10.1159/000121368.

38. Tagin, M.A., Woolcott, C.G., Vincer, M.J., Whyte, R.K., and Stinson, D.A. (2012). Hypothermia for neonatal hypoxic ischemic encephalopathy: an updated systematic review and meta-analysis. *Arch Pediatr Adolesc Med* 166(6), 558-566. doi: 10.1001/archpediatrics.2011.1772.

39. Ten, V.S., Wu, E.X., Tang, H., Bradley-Moore, M., Fedarau, M.V., Ratner, V.I., et al. (2004). Late measures of brain injury after neonatal hypoxia-ischemia in mice. *Stroke* 35(9), 2183-2188. doi: 10.1161/01.STR.0000137768.25203.df.

40. Wang, H., Wang, L., Li, N.L., Li, J.T., Yu, F., Zhao, Y.L., et al. (2014). Subanesthetic isoflurane reduces zymosan-induced inflammation in murine Kupffer cells by inhibiting ROS-activated p38 MAPK/NF-κB signaling. *Oxid Med Cell Longev* 2014, 851692. doi: 10.1155/2014/851692.

41. Wang, W.T., Sun, Y.M., Huang, W., He, B., Zhao, Y.N., and Chen, Y.Q. (2016). Genome-wide Long Non-coding RNA Analysis Identified Circulating LncRNAs as Novel Non-invasive Diagnostic Biomarkers for Gynecological Disease. *Sci Rep* 6, 23343. doi: 10.1038/srep23343.

42. Xiong, L., Zheng, Y., Wu, M., Hou, L., Zhu, Z., Zhang, X., et al. (2003). Preconditioning with isoflurane produces dose-dependent neuroprotection via activation of adenosine triphosphate-regulated

potassium channels after focal cerebral ischemia in rats. *Anesth Analg* 96(1), 233-237, table of contents. doi: 10.1097/00000539-200301000-00047.

43. Yan, W., Chen, Z., Chen, J., and Chen, H. (2016). Isoflurane preconditioning protects rat brain from ischemia reperfusion injury via up-regulating the HIF-1α expression through Akt/mTOR/s6K activation. *Cell Mol Biol (Noisy-le-grand)* 62(2), 38-44.
44. Yang, B., Xia, Z.A., Zhong, B., Xiong, X., Sheng, C., Wang, Y., et al. (2017). Distinct Hippocampal Expression Profiles of Long Non-coding RNAs in an Alzheimer's Disease Model. *Mol Neurobiol* 54(7), 4833-4846. doi: 10.1007/s12035-016-0038-5.
45. Yang, Y., Chen, L., Si, J., Ma, K., Yin, J., Li, Y., et al. (2020). TGF-β3/Smad3 Contributes to Isoflurane Postconditioning Against Cerebral Ischemia-Reperfusion Injury by Upregulating MEF2C. *Cell Mol Neurobiol* 40(8), 1353-1365. doi: 10.1007/s10571-020-00822-5.
46. Yao, Z., Liu, N., Zhu, X., Wang, L., Zhao, Y., Liu, Q., et al. (2020). Subanesthetic isoflurane abates ROS-activated MAPK/NF-κB signaling to repress ischemia-induced microglia inflammation and brain injury. *Aging (Albany NY)* 12(24), 26121-26139. doi: 10.18632/aging.202349.
47. Zhao, D.A., Bi, L.Y., Huang, Q., Zhang, F.M., and Han, Z.M. (2016). [Isoflurane provides neuroprotection in neonatal hypoxic ischemic brain injury by suppressing apoptosis]. *Rev Bras Anestesiol* 66(6), 613-621. doi: 10.1016/j.bjan.2016.08.003.
48. Zimin, P.I., Woods, C.B., Kayser, E.B., Ramirez, J.M., Morgan, P.G., and Sedensky, M.M. (2018). Isoflurane disrupts excitatory neurotransmitter dynamics via inhibition of mitochondrial complex I. *Br J Anaesth* 120(5), 1019-1032. doi: 10.1016/j.bja.2018.01.036.

Figures

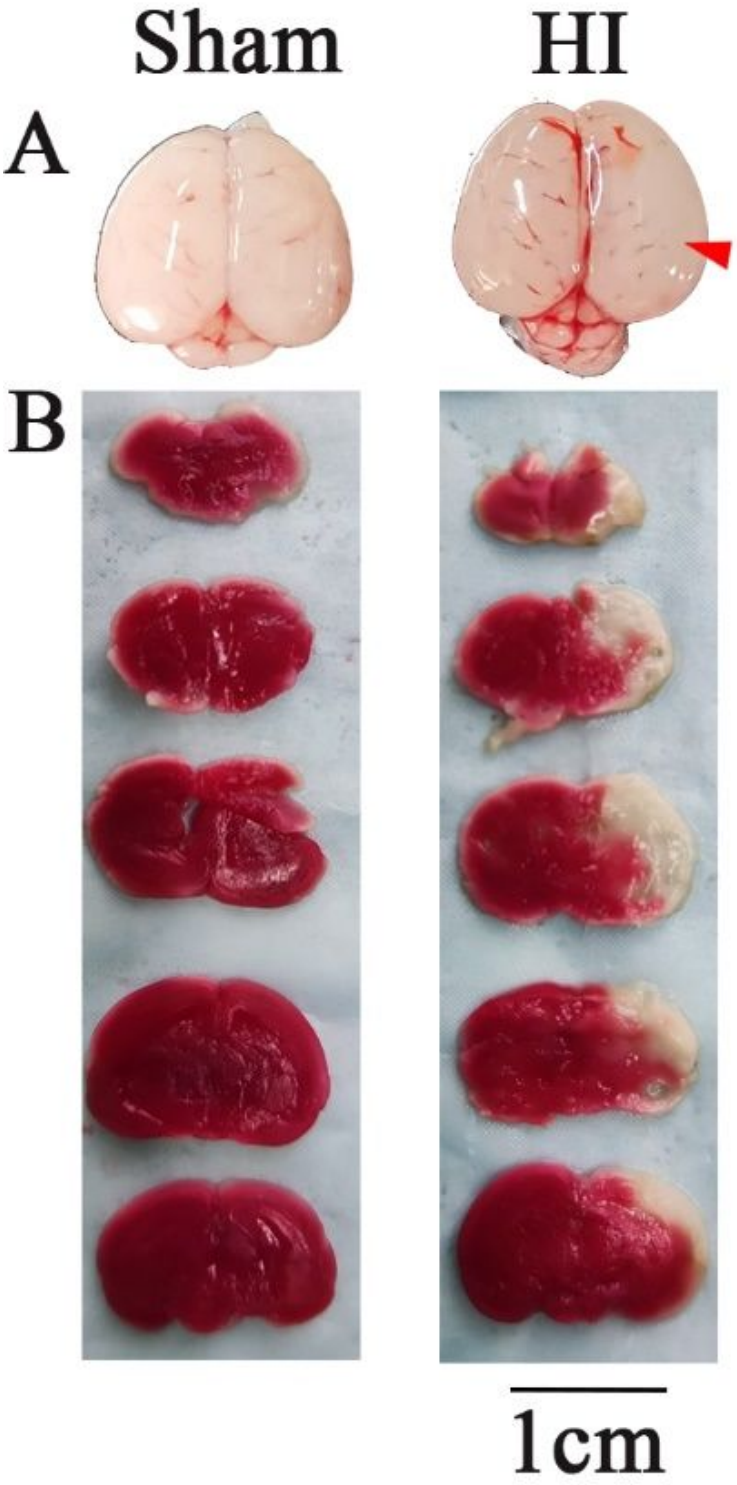

Figure 1

TTC staining among the sham, HI groups at 24 h after HI. (A) anatomic appearance of brain tissues. (B) TTC staining. Scale bar = 1 cm. Pale white represents the infarct area, red shows the normal staining.

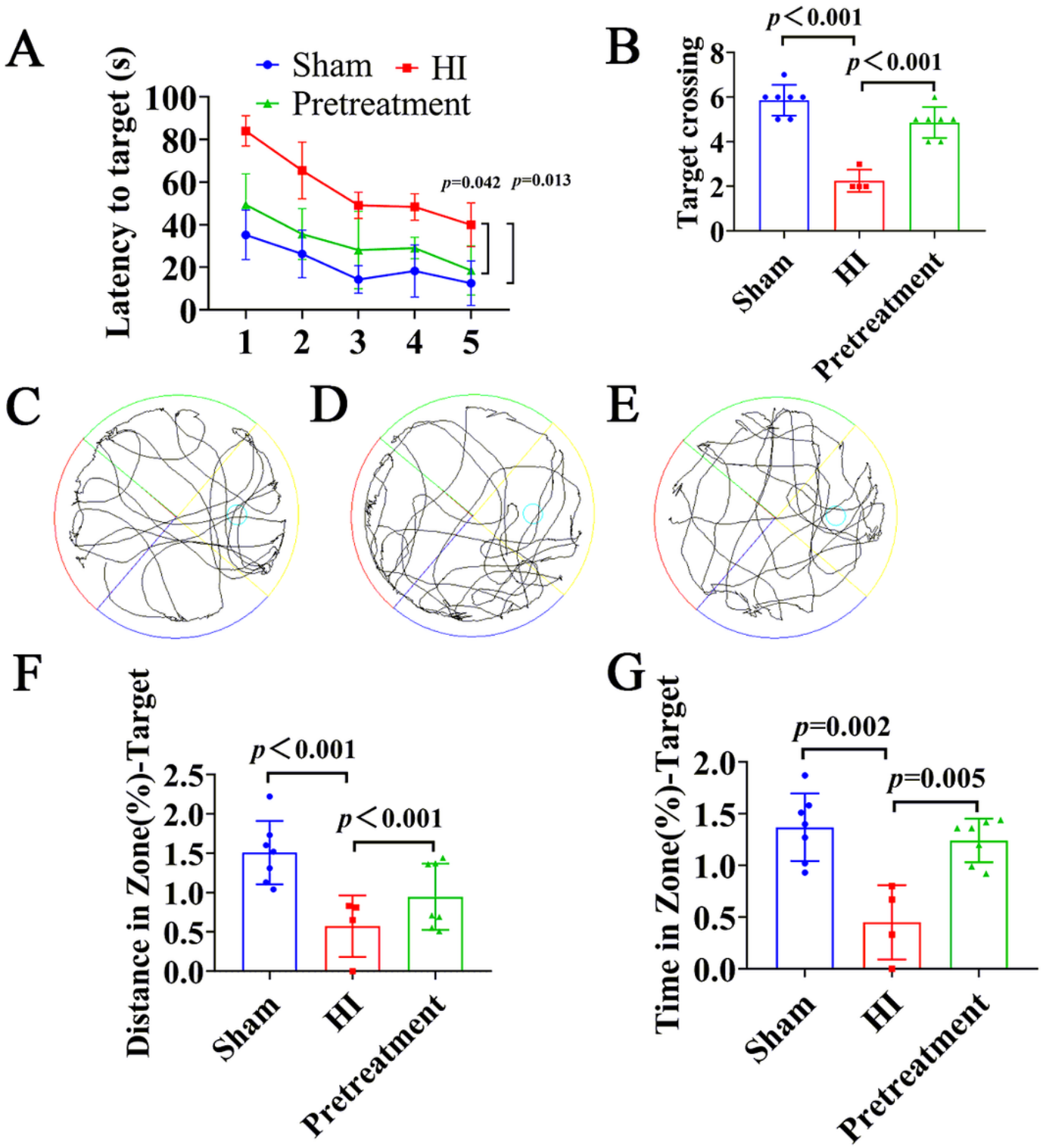

Figure 2

Morris water maze test in rats after isoflurane pretreatment. (A) Five-day escape latency in rats. HI vs. Sham group, p = 0.013; Pretreatment group vs. HI group, p = 0.042. (B) Number of target platform crossing on the sixth day. (C-E) The trajectory maps of rats in the sham, HI, and Pretreatment groups, respectively. (F-G) The percentage of distance and time of the target quadrant to all quadrants.

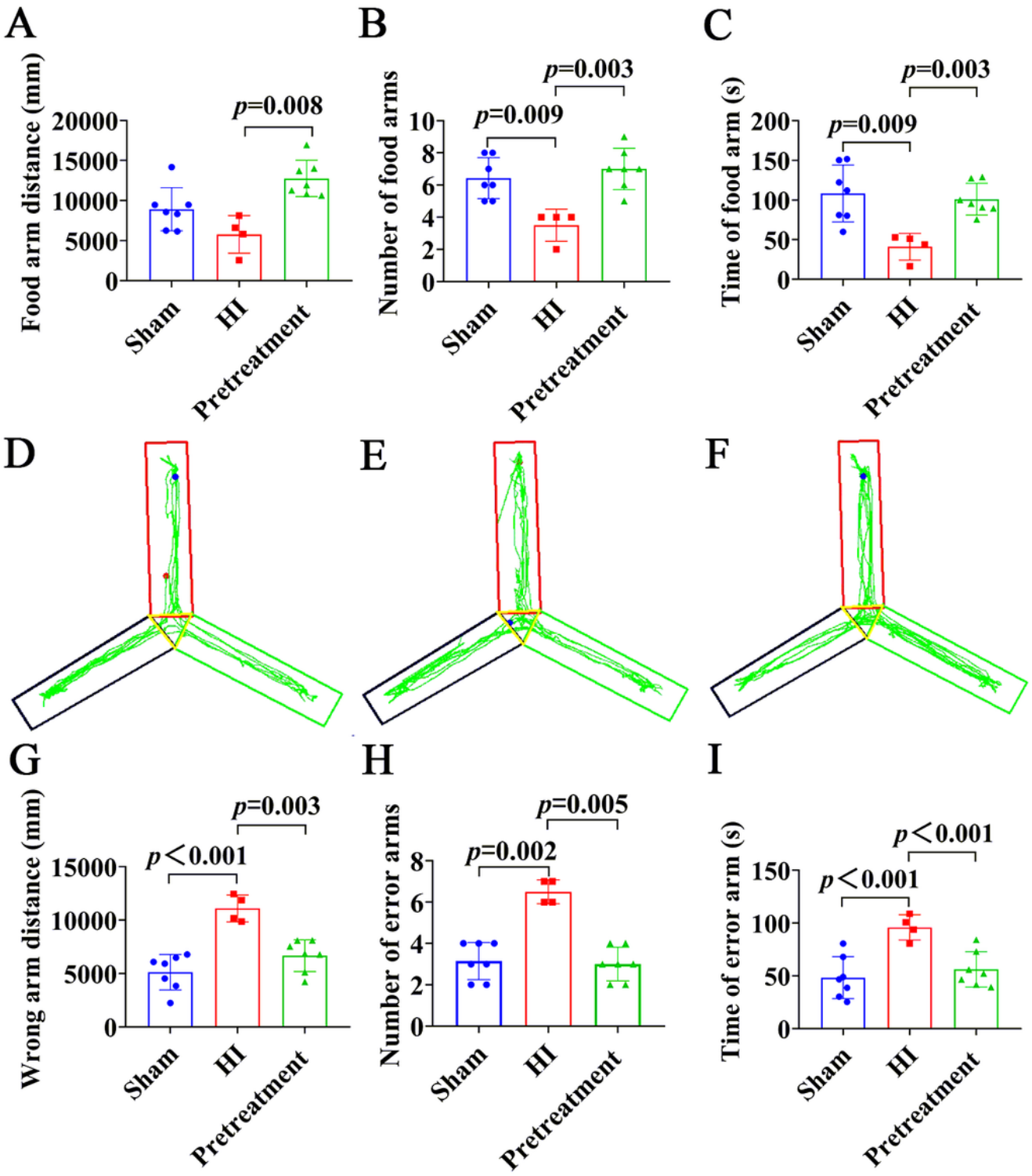

Figure 3

Y-maze test in rats after isoflurane pretreatment. (A-C) Walking distance, number of entries, and duration in the food arm for Sham, HI, and Pretreatment rats, respectively. (D-F) The walking trajectory maps of rats in the sham, HI, and Pretreatment groups, respectively. The start arm was on the above, the wrong arm was on the left, and the food arm was on the right. (G-I) The walking distance, number of entries, and duration of Sham, HI, and Pretreatment rats on the wrong arm, respectively.

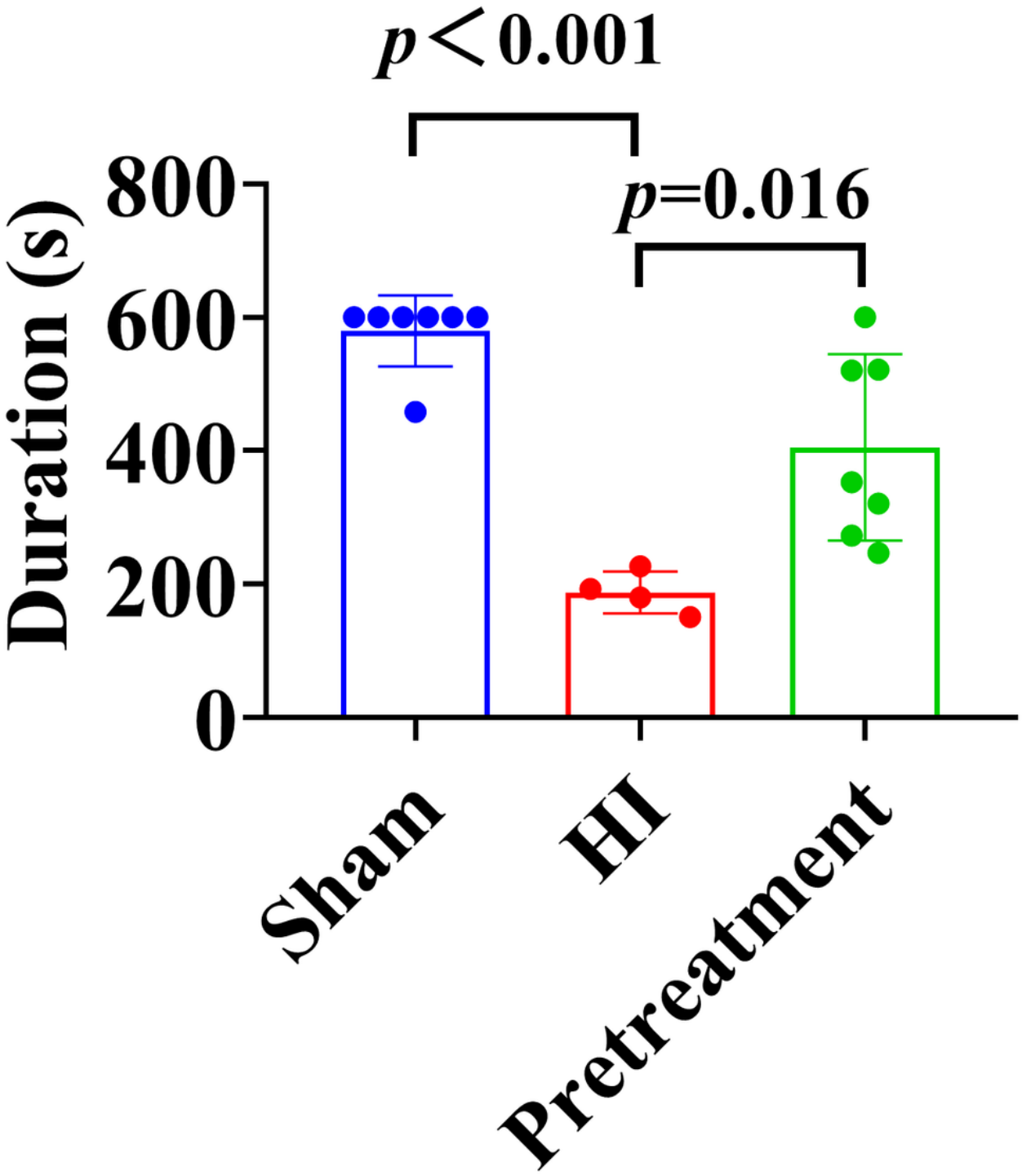

Figure 4

Duration of rats on the rotarod in the rotarod test.

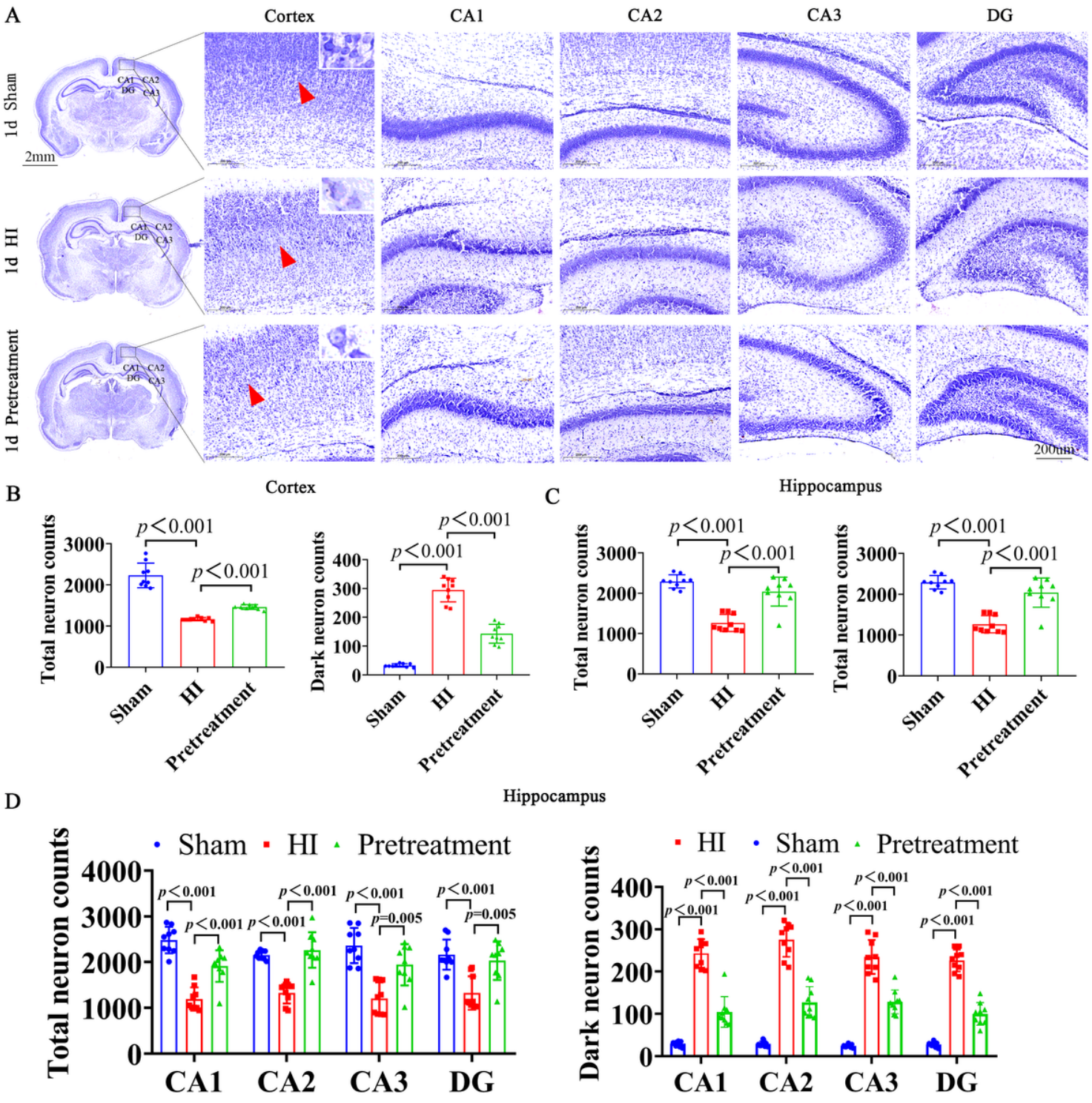

Figure 5

Nissl staining of neonatal HI 1 d rats treated with pretreatment. (A) Three images on the left are the brain appearance of sham, HI and Pretreatment groups. Scale bar = 2mm. The black box represents the right cortex and hippocampus CA1, CA2, CA3, and DG. Scale bar = 200 μm. The red arrow shows the cell. (B) The number of total neurons in sham, HI and Pretreatment groups in the cortex and hippocampus. (C) The number of dark neurons in sham, HI and Pretreatment groups in the cortex and hippocampus. Scale

bar = 200 μm. (D) Quantitative histograms of total neurons and dark neurons in the hippocampal CA1, CA2, CA3, DG. Data are presented as mean ± SD.

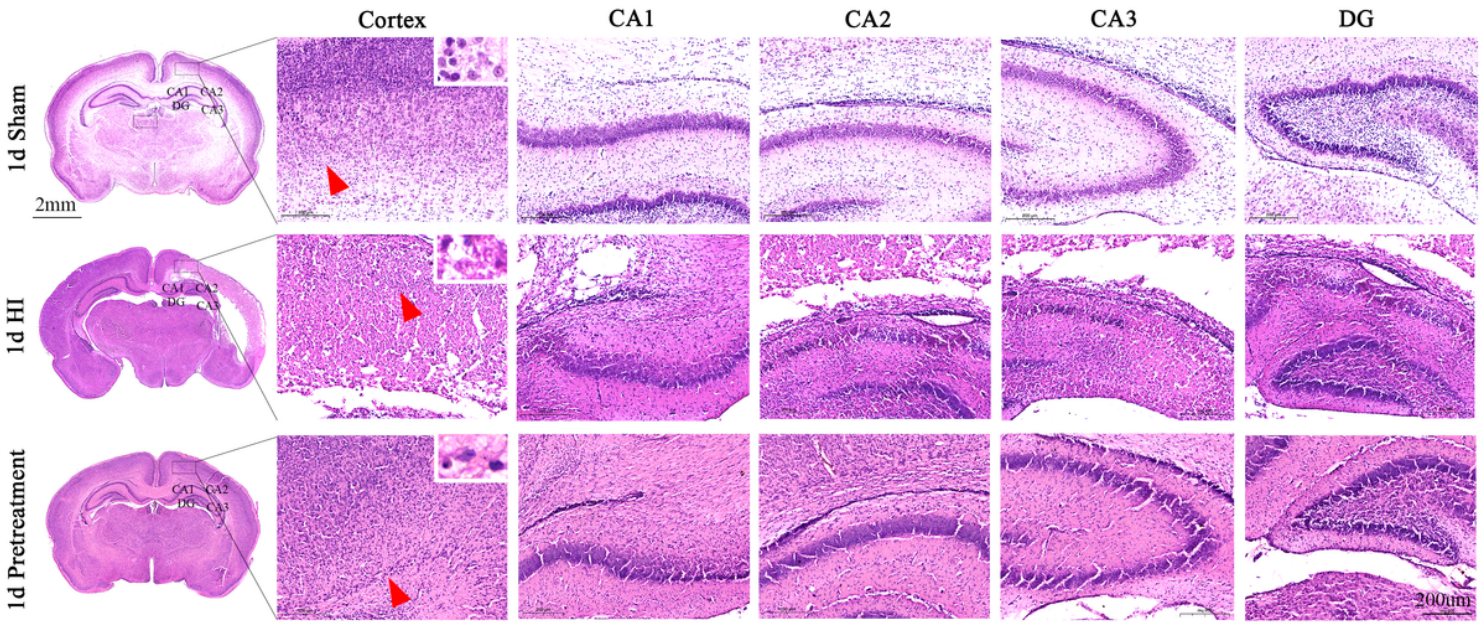

Figure 6

HE staining of neonatal HI1 d rats treated with Pretreatment. (A) Three images on the left are the brain appearance of sham, HI and Pretreatment groups. Scale bar = 2 mm. The black box represents the right cortex and hippocampus. Scale bar = 200 μm.

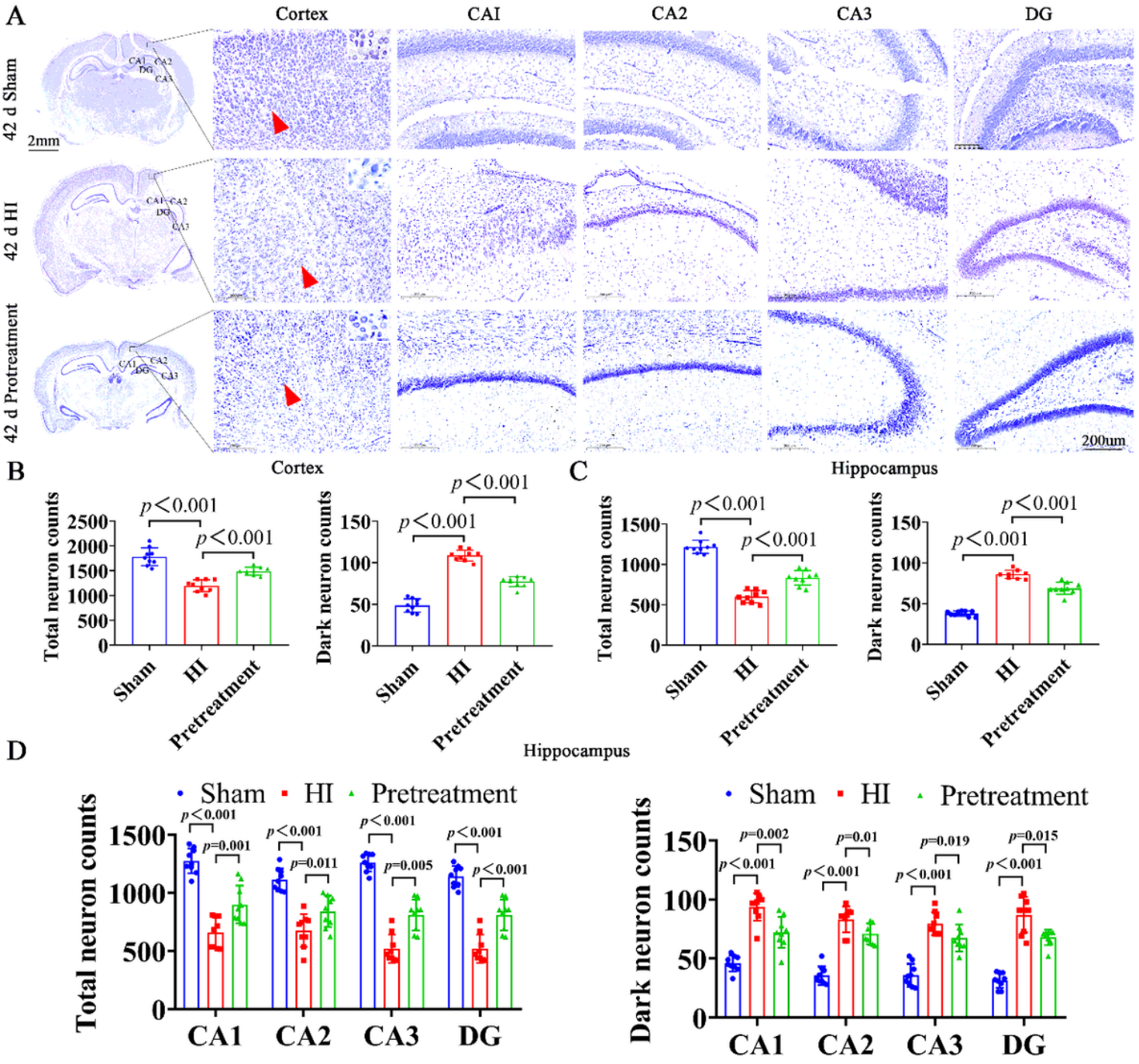

Figure 7

Nissl staining of neonatal HI42 d rats treated with pretreatment. (A) Three images on the left are the brain appearance of sham, HI and Pretreatment groups. Scale bar = 2mm. The black box represents the right cortex and hippocampus CA1, CA2, CA3, and DG. Scale bar = 200 μm. The red arrow shows the cell. (B) The number of total neurons in sham, HI and Pretreatment groups in the cortex and hippocampus. (C) The number of dark neurons in sham, HI and Pretreatment groups in the cortex and hippocampus. Scale bar = 200 μm. (D) Quantitative histograms of total neurons and dark neurons in the hippocampal CA1, CA2, CA3, DG. Data are presented as mean ± SD.

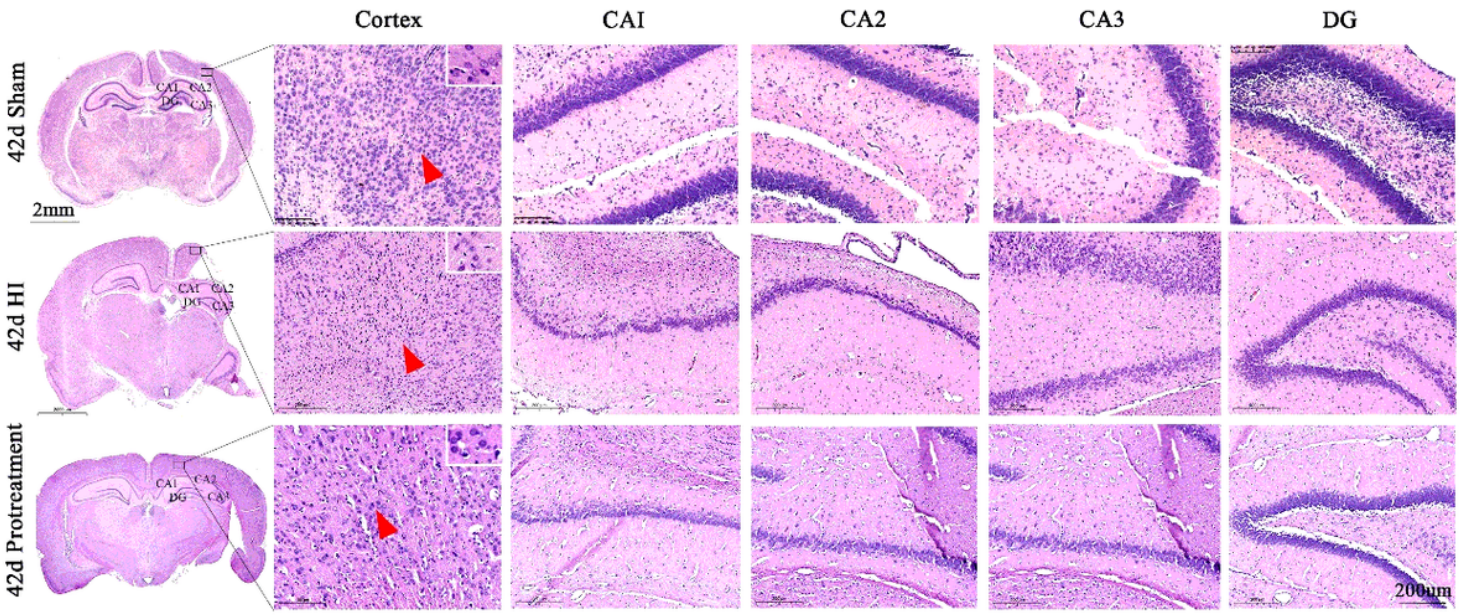

Figure 8

HE staining of neonatal HI 42 d rats treated with Pretreatment. (A) Three images on the left are the brain appearance of sham, HI and Pretreatment groups. Scale bar = 2 mm. The black box represents the right cortex and hippocampus. Scale bar = 200 μm.

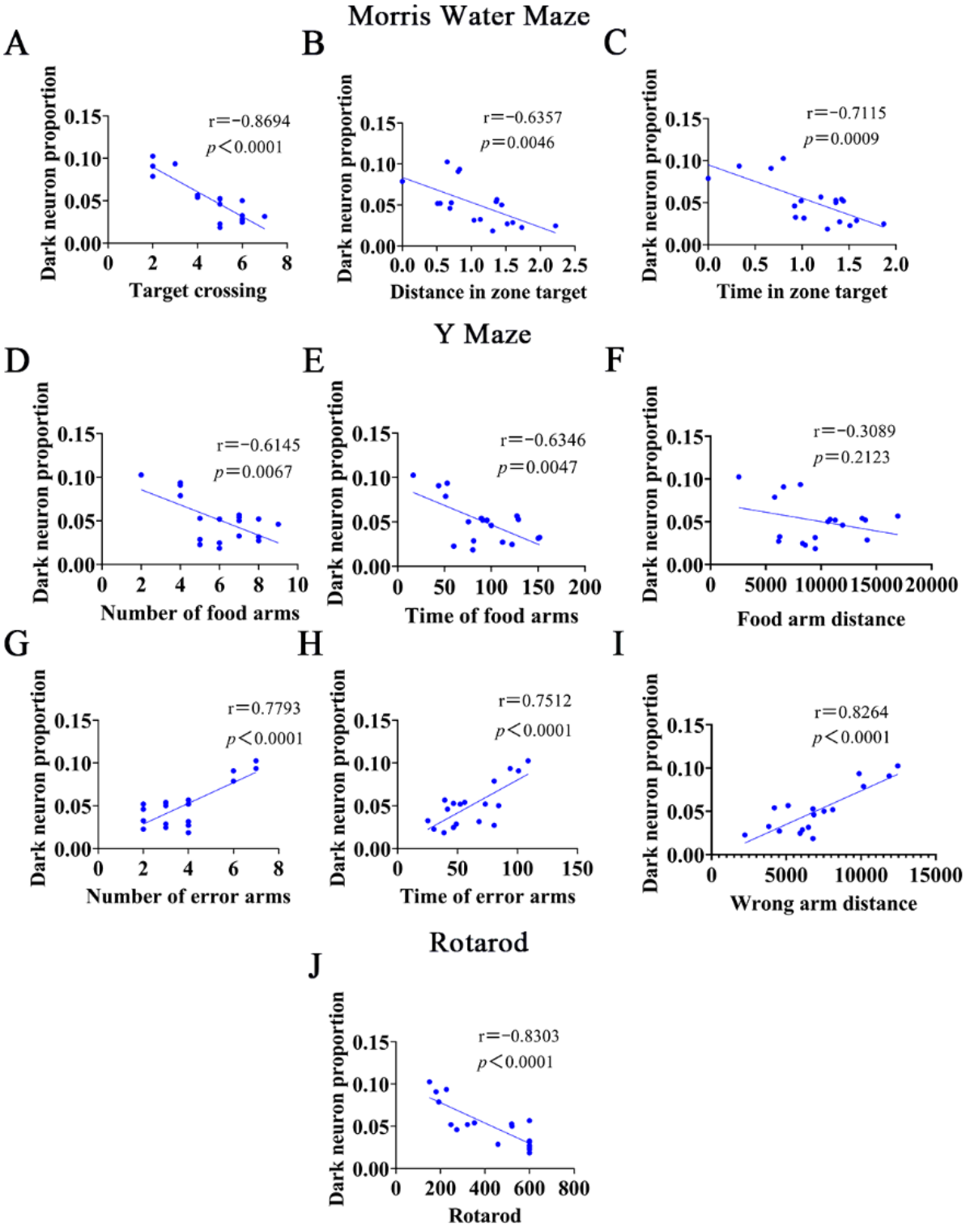

Figure 9

Correlation analysis between the percentage of Dark neuron to Total neuron, a behavioral index, and each index of morphology in HI rats after isoflurane pretreatment. (A-C) The correlation analysis between morphology and the number of passes, the percentage of distance from the target quadrant, and the percentage of morphology of the water maze, respectively（D-I) The correlation analysis between

morphology and the number of food arm entries, duration, distance, number of wrong arm entries, duration, and distance in the Y-maze. (J) The correlation analysis between morphology and rotarod.